UWL REPOSITORY

repository.uwl.ac.uk

Strength, Durability, and Microstructural Characteristics of Binary Concrete Mixes Developed with Ultrafine Rice Husk Ash as Partial Substitution of Binder.

This is the Published Version of the final output.

Alternative formats: If you require this document in an alternative format, please contact: open.research@uwl.ac.uk

Strength, Durability, and Microstructural Characteristics of Binary Concrete Mixes Developed with Ultrafine Rice Husk Ash as Partial Substitution of Binder

Roz-Ud-Din Nassar[1,*], Shah Room[2]

[1]Department of Civil and Infrastructure Engineering, American University of Ras Al Khaimah, United Arab Emirates
[2]Department of Civil and Environmental Engineering, University of West London, UK

Abstract This study investigates the utilization of ultrafine Rice Husk Ash (RHA) as a partial replacement for cement in concrete to enhance its properties and sustainability. The effects of ultrafine RHA on fresh and hardened concrete properties and the microstructure of the resulting binary mixtures were examined. Test results indicate that the incorporation of ultrafine RHA considerably decreases the slump of concrete mixtures. Mixture having 15% replacement of cement with ultrafine RHA shows a 43% increase in compressive strength at 90 days of concrete age. Furthermore, at the same replacement level, a 31% reduction in moisture sorption, a 27% reduction in drying shrinkage, and a 23% reduction in mass loss due to abrasion are recorded. Acid resistance tests show that the mix with 15% ultrafine RHA loses only 12% of its compression strength after exposure to H_2SO_4 at 56 days of age, in comparison to the 29% loss in the control mix. SEM, EDX, and XRD analyses confirm a denser microstructure, increased silica content, and enhanced pozzolanic activity in ultrafine RHA-modified mixes. These findings suggest that ultrafine RHA is a viable supplementary cementitious material, offering significant environmental and performance benefits to the resulting concrete mixtures.

Keywords Rice Husk Ash, Concrete Durability, Pozzolanic Reaction, Compressive Strength, Sustainable Construction

1. Introduction

The durability of hardened concrete is as critical as its strength in ensuring the prolonged service life of built infrastructure. Key durability attributes of concrete include its moisture barrier characteristics, reduced drying shrinkage, acid resistance, and enhanced abrasion resistance [1, 2]. Among these, resistance to moisture transport is particularly crucial, as it directly affects the drying shrinkage of concrete, which in turn is governed by the microstructure of the material [3, 4]. Concrete mixtures characterized by a dense microstructure and reduced porosity exhibit superior resistance to dimensional changes, specifically drying shrinkage. This is because such mixtures hinder moisture transport more effectively. Structural members in buildings, which are typically restrained at their joints with other members, are not free to expand or contract. Consequently, excessive dimensional changes can lead to cracking in these members [5-7]. Therefore, minimizing the drying shrinkage of concrete is

of paramount importance for enhancing the durability and extending the service life of the structures it composes. The moisture barrier characteristics of concrete also play a significant role in its overall durability, as many deterioration processes are initiated by the ingress of harmful ions, which use water as a vehicle to penetrate the concrete matrix [8, 9]. To mitigate this, it is essential to perform pore filling and pore refinement within the microstructure of cementitious materials, thereby improving their water barrier properties [10, 11].

Various factors influence the microstructural properties of concrete, such as the water-to-cement ratio, the use of supplementary cementitious materials (SCMs), and the type of aggregate used [12, 13]. A lower water-to-cement ratio generally leads to a denser microstructure with reduced porosity, which enhances the moisture barrier characteristics of the concrete. SCMs, such as fly ash, silica fume, and slag, contribute to the refinement of the pore structure by filling voids and producing additional cementitious compounds through pozzolanic reactions [14, 15]. The use of pozzolanic materials, whether derived from industrial byproducts or agricultural wastes, significantly enhances the impermeability of concrete. This improvement is achieved through the production of additional solid-phase products that contribute to the pore-filling effect in the microstructure of concrete, thereby improving the moisture transport characteristics of the resulting mixtures [16, 17]. Moreover, the incorporation of these materials as partial replacements for cement in concrete has been observed to substantially enhance the strength and durability attributes of the resulting concrete mixtures [8, 9].

Cement production, the primary component of concrete, is inherently environmentally polluting, with every ton of OPC development resulting in approximately 0.9 tonnes of CO_2 emissions into the atmosphere [18, 19]. Additionally, cement production is an energy-intensive process [15, 16]. This situation necessitates urgent attention to mitigate the adverse environmental impacts of cement production [20, 21]. Agricultural wastes, which are predominantly biodegradable, can be beneficially utilized in concrete once they are burnt under controlled temperatures and pulverized to fine particle sizes. The incinerated residue of most agricultural wastes is rich in free silica and alumina, making it suitable for use in concrete to produce binary concrete mixtures. The literature documents the addition of various processed agriculture discarded materials as fractional replacements for OPC, resulting in the production of environmentally friendly and durable concrete mixtures [22, 23]. Previous research has reported significant energy and environmental benefits, in addition to enhanced strength and durability, from the use of various agricultural byproducts as partial replacements for cement in concrete [24, 25]. These findings underscore the potential of agricultural wastes to not only contribute to sustainable construction practices but also to enhance the properties of concrete.

The annual global rice production, which has reached 742 million metric tons, generates approximately 148 million metric tons of rice husk [26]. The disposal of rice husks is typically managed in environmentally harmful ways, such as dumping them in open areas, which not only occupies land but also disrupts the ecosystem. Additionally, burning rice husks in open areas contaminates groundwater and contributes to environmental degradation [20]. The regional production of rice husk reflects the global significance of this agricultural byproduct. In the United States, rice production in 2022 was approximately 7.1 million metric tons, resulting in around 1.42 million metric tons of rice husk annually. India, as one of the largest rice producers, generated about 130 million metric tons of rice in 2022, translating to approximately 26 million metric tons of rice husk. Europe, with primary producers like Italy and Spain, had a total rice production of about 4.1 million metric tons in 2022, producing roughly 0.82 million metric tons of rice husk. China, the world leader in rice production, produced about 212 million metric tons of rice in 2022, resulting in approximately 42.4 million metric tons of rice husk annually [27, 28].

However, suitable pretreatment, such as burning rice husk under controlled temperatures, can convert the silica in the husk to amorphous silica, which possesses significant pozzolanic reactivity [29, 30]. The resulting incinerated rice husk, known as Rice Husk Ash (RHA), is not only chemically active but also has favorable properties for use in concrete as a partial substitute for cement [31]. The utilization of RHA in concrete not only provides a sustainable solution for rice husk disposal but also enhances the durability and strength characteristics of concrete. By integrating RHA, the construction industry can contribute to reducing environmental impacts associated with cement production and rice husk disposal while promoting the development of more sustainable building materials. The beneficial effects of incorporating RHA in concrete mixtures include enhanced strength and durability, as well as a reduction in drying shrinkage compared to concrete mixtures produced solely with cement [32, 33]. These advantages stem from the pozzolanic reaction of RHA, which contributes to the formation of additional cementitious compounds, thereby refining the microstructure of concrete and improving its performance characteristics.

The present study reports the findings of an experimental investigation carried out on the production of concrete by partially replacing cement with ultrafine RHA. Ultrafine RHA, distinguished from normal RHA by its finer particle size and higher reactivity, offers enhanced pozzolanic properties due to its increased surface area. This enhanced reactivity facilitates better bonding within the concrete matrix, contributing to improved mechanical and durability characteristics. The investigation focused on assessing the strength and durability characteristics of the resulting sustainable concrete mixtures through a series of comprehensive tests. These tests included compression

strength, water absorption, drying shrinkage, resistance against acid and abrasion, and Scanning Electron Microscopy (SEM) analysis, Energy Dispersive X-ray (EDX) analysis, and X-ray Diffraction (XRD) analysis. When compared to conventional concrete mixtures produced with 100% cement as the binder material, the ultrafine RHA-blended mixtures demonstrated promising results. The inclusion of ultrafine RHA in the concrete mix not only provided comparable or enhanced compressive strength but also significantly improved durability attributes such as reduced moisture sorption, lower drying shrinkage, enhanced abrasion resistance, and increased acid resistance.

2. Materials and Methods

In this study, all concrete mixtures were prepared using Ordinary Portland Cement (OPC), meeting the standards of ASTM C150 [34]. The aggregates comprised limestone with a maximum size of 13 mm and natural sand with a fineness modulus of 2.45. Tap water and a superplasticizer (SP) with a specific gravity of 1.03 were also included. Ultrafine rice husk ash (RHA), with a specific gravity of 2.15 g/cm³, was produced by incinerating raw rice husk under controlled temperature conditions. Figure 1 illustrates the raw rice husk and the processed RHA powder. The scanning electron microscope (SEM) image (Figure 2) reveals that the ultrafine RHA particles are irregularly shaped and display a wide range of sizes. Table 1 details the chemical composition of the OPC and ultrafine RHA used in this study, while Table 2 provides the physical properties of the coarse and fine aggregates.

The particle size distribution of PC and ultrafine RHA is illustrated in Figure 3. The graph demonstrates that ultrafine RHA particles exhibit a significantly finer distribution compared to PC. The cumulative size distribution curve for RHA shifts to the left, indicating a higher proportion of smaller particles. Specifically, the median particle size (D50) for RHA is approximately 0.4 μm, whereas for PC, it is around 2 μm. This finer particle size of ultrafine RHA, with a substantial portion of particles below 1 μm, contributes to its higher reactivity and pozzolanic activity, facilitating improved bonding and enhanced performance in concrete mixtures. The distribution also shows that nearly 100% of RHA particles are below 10 μm, in contrast to OPC, which has a broader size range extending to larger particles. This finer distribution is instrumental in achieving the enhanced mechanical and durability properties observed in RHA-blended concrete. Four concrete mixtures were prepared, including a control mixture and three binary mixtures where OPC was partially replaced with ultrafine RHA at 5%, 10%, and 15% by weight. The control mixture contained only OPC as the binder. The composition of the four mixtures is detailed in Table 3.

(a)

(b)

Figure 1. Views of: (a) Rice Husk and (b) Ultrafine Powdered RHA
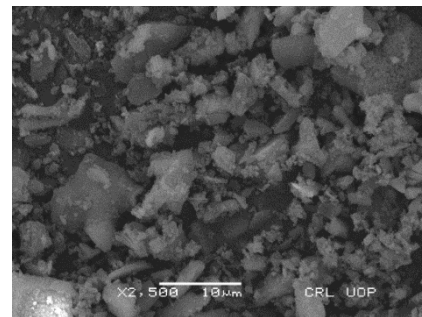
Figure 2. SEM Image of Ultrafine RHA used in the Experimental Program

Table 1. Chemical composition of OPC and RHA

Compound	RHA	OPC
	(% mass)	
SiO_2	90.66	21.52
Al_2O_3	0.71	5.93
CaO	0.59	62.75
Fe_2O_3	0.19	3.89
MgO	0.55	2.2
K_2O	6.68	0.90
Na_2O	0.04	0.18
SO_3	0.58	2.63
LOI	-	2.91

Table 2. Physical Characteristics of Fine and Coarse Aggregates

Aggregate type	Dry density (kg/m^3)	Loss on abrasion (%)	Fineness modulus	Bulk specific gravity	Absorption (%)	Fineness modulus	Bulk specific gravity (SSD)
Fine aggregates	1620.34	-	2.45	2.59	0.91	2.45	-
Coarse	1765.56	18.87	-	2.58	2.25	-	2.69

Figure 3. Particle size distribution of RHA and PC

Table 3. Composition of concrete mixtures

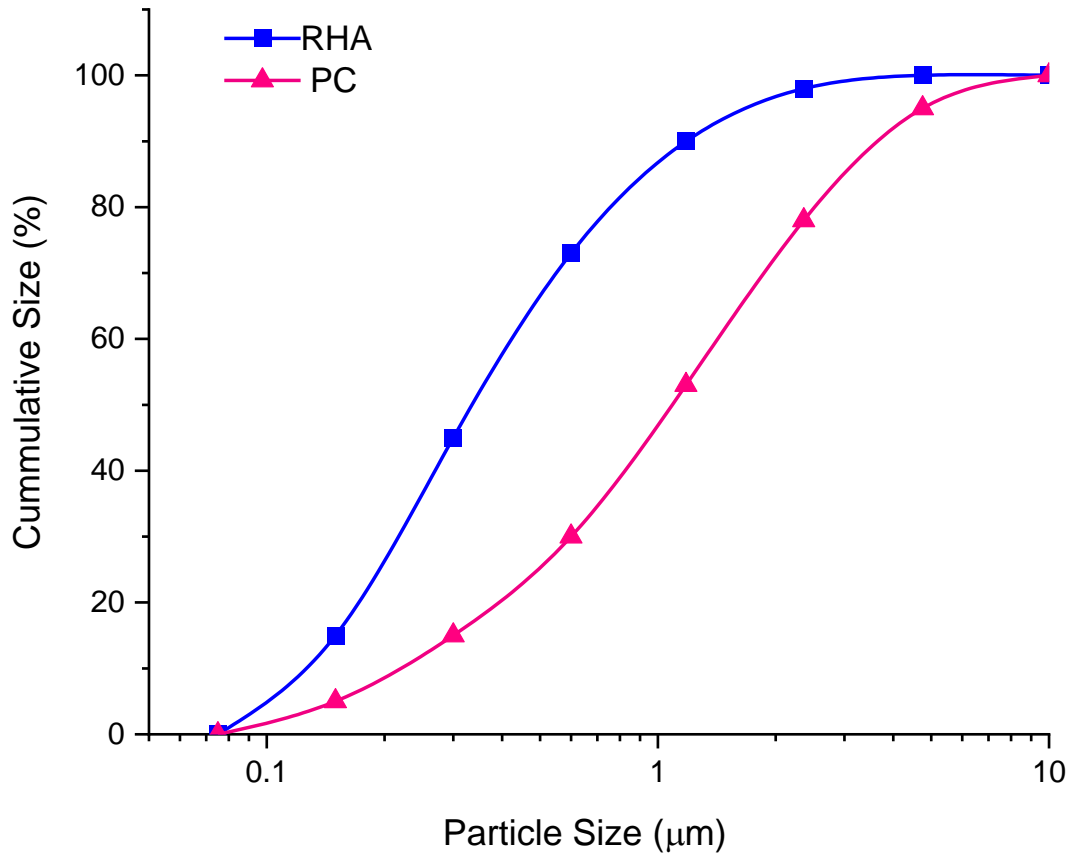| Mix ID	Fine aggregates (kg/m^3)	Coarse aggregates (kg/m^3)	W/C$^\#$ ratio	OPC (kg/m^3)	Water (kg/m^3)	RHA (kg/m^3)	SP (ml/kg)
M1*	628.73	937.81	0.41	463.62	190.55	-	2.34
M2	628.73	937.81	0.41	430.52	190.55	33.10	2.34
M3	628.73	937.81	0.41	397.42	190.55	66.20	2.34
M4	628.73	937.81	0.41	364.32	190.55	99.30	2.34

*control mixture $^\#$ water to cementitious ratio

All concrete mixtures were prepared using a standard laboratory mixer to ensure uniformity. Cylinder specimens measuring 100 mm in diameter and 200 mm in height were cast for compressive strength and acid resistance tests. Additionally, 50 mm thick discs, cut from the cylinder specimens after 28 days of curing, were used for water sorption and abrasion resistance tests. These disc specimens were dried in an oven until a constant mass was achieved. Then, the samples were wrapped from the top and it sides with epoxy to facilitate a 1D sorption phenomenon. Sorption was quantified by measuring the variance in mass, which was then divided by the product of the X-sectional area of the samples and the water's density (0.001 g/mm³), yielding results in units of length (mm).

Concrete prisms with a square cross-section of 75 mm and a length of 286 mm were prepared according to the procedures described in ASTM C192 [36] for the drying shrinkage test. After an initial comparator reading at 24 hours, the specimens were cured in tap water. The drying shrinkage tests were conducted in accordance with ASTM C157 and ASTM C490 [37] guidelines. To assess acid resistance, both control and binary concrete mixtures were subjected to a 0.1 M H_2SO_4 solution for 56 days following ASTM C1898 [38]. The specimens, aged 28 days, were exposed to the acidic solution, and their loss in compressive strength was measured at intervals of 7, 14, 28, and 56 days. All specimens were maintained in water at a temperature of 25 ± 2 ℃ until the designated test ages. For each concrete mixture, three specimens were prepared, and the results represent the average of three readings. The water sorption test involved drying the disc specimens to a constant mass, followed by epoxy sealing to restrict sorption to a single dimension. Sorption was then measured by recording the mass change over time. The abrasion resistance test utilized the same discs, subjected to standardized abrasion testing to determine the material's durability under wear.

For Scanning Electron Microscopy analysis, small samples were extracted from the fractured surfaces of the concrete cylinders after compressive strength testing. These samples were further reduced in size to approximately 10 mm x 10 mm x 10 mm to fit the SEM specimen holder. The samples were then dried in an oven at 60 ℃ for 24 hours to remove any residual moisture. Once dried, the samples were mounted on aluminum stubs using conductive carbon tape. To ensure proper imaging, the mounted samples were sputter-coated with a thin layer of gold-palladium alloy to improve conductivity. SEM imaging was performed at magnifications of 100x and 1000x to observe the microstructure and identify the distribution of hydration products, pores, and cracks.

Energy Dispersive X-ray analysis was conducted in conjunction with SEM. The same samples used for SEM were analyzed for their elemental composition. EDX spectra were collected at multiple points on each sample to ensure a representative analysis of the material's composition. The EDX detector was calibrated using a standard sample, and the analysis was performed under high vacuum conditions with an accelerating voltage of 15 kV. The elemental peaks in the EDX spectra were identified and quantified to determine the presence and relative abundance of elements such as calcium, silicon, aluminum, and other trace elements.

For X-ray Diffraction analysis, powdered samples were prepared from the concrete cylinders. Small fragments of the concrete were ground using a mortar and pestle to obtain a fine powder. The powder was then passed through a 75 μm sieve to ensure uniform particle size. The powdered samples were placed on a flat sample holder, and a smooth surface was obtained by gently pressing the powder with a glass slide. XRD measurements were performed using a diffractometer with Cu-Kα radiation (λ = 1.5406 Å). The scanning range was set from $10°$ to $80°$ 2θ with a step size of 0.02° and a scanning speed of 1° per minute. The diffraction patterns were analyzed to identify the crystalline phases present in the samples. Peaks corresponding to calcium hydroxide, calcium silicate hydrate, silica, and other relevant phases were identified using standard reference patterns.

3. Results and Discussion

3.1. Fresh Characteristics

Table 4 presents the fresh concrete test results of all mixtures. It is noted that with an increase in the partial replacement of cement with ultrafine RHA, the slump (workability) of the mixture drops compared to the control mixture. This trend can be explained by the ultrafine nature of RHA, which significantly influences the properties of fresh concrete. The tiny particles of ultrafine RHA result in a large surface area, which increases the water demand of the blended binder and consequently reduces the workability (slump) of the mixture. The large surface area necessitates more water to achieve the same level of lubrication between particles as in a mixture without RHA. Moreover, the lower specific gravity of ultrafine RHA compared to cement leads to a higher number of particles per unit mass of concrete, further increasing the water requirement to wet the particles adequately.

Table 4. Fresh Characteristics of Binary Concrete

| Mix ID	Workability (cm)	Temperature (ºC)	Freshly mixed Unit Wt (kg/m^3)
M1	8	24.0	2819
M2	7	25.0	2790
M3	5	24.5	2757
M4	5	24.5	2731

Additionally, the reduction in workability with increased ultrafine RHA content can be attributed to the angular shape of ultrafine RHA particles. These particles tend to interlock more easily, reducing the fluidity of the mixture. This interlocking effect, combined with the higher surface area, results in a stiffer mixture that is less workable. Therefore, it is essential to adjust the mix design to maintain adequate workability for proper placement and compaction of the concrete when using ultrafine RHA. Table 4 also indicates that with an increase in ultrafine RHA dosage, the fresh concrete density of the binary concrete mixtures decreases. This trend is due to the lightweight nature of ultrafine RHA particles compared to the relatively heavier cement particles in the control mixture. Consequently, the binary mixtures with higher RHA content exhibit lower fresh concrete density in comparison to the reference mixture [39].

The decline in density of fresh concrete with higher ultrafine RHA content has practical implications. Lower density can be advantageous in lowering the overall weight of the structure, which is particularly advantageous in load-bearing applications where weight reduction can lead to cost savings in structural support requirements. However, it is crucial to balance this benefit with the potential influence on the strength characteristics of the final concrete. Incorporating ultrafine RHA into concrete not only addresses environmental concerns related to the disposal of rice husks but also contributes to sustainable construction practices by reducing the reliance on traditional cement [35]. The observed trends in workability and density are consistent with findings from other studies, which have shown similar effects of pozzolanic materials on fresh concrete properties. The enhanced sustainability and performance characteristics of ultrafine RHA-blended concrete underscore its potential as a viable alternative in the construction industry.

3.2. Compressive Strength

Figure 4 presents the compression strength (CS) of all mixes at 7, 28, and 90 days of curing. At curing of 7 days, the reference mixture (M1) displays high CS compared to the binary concrete mixtures (M2, M3, M4). This early-age strength reduction in the binary mixtures is caused by the dilution effect, wherein part of the Portland cement is replaced with ultrafine RHA. At this early stage of

hydration, ultrafine RHA remains largely inert, much like other supplementary cementitious materials. However, at 28 days of concrete age and beyond, the compressive strength trends shift favorably towards the binary mixtures. This change is primarily attributed to the pozzolanic reaction of ultrafine RHA with the hydration products of Portland cement, particularly calcium hydroxide. The pozzolanic activity of ultrafine RHA converts calcium hydroxide into calcium silicate hydrate (C-S-H), which significantly improves the strength and stability of the hydrated concrete mixtures [27]. This reaction not only densifies the microstructure but also reduces the presence of free lime, which is beneficial for the long-term durability of the concrete.
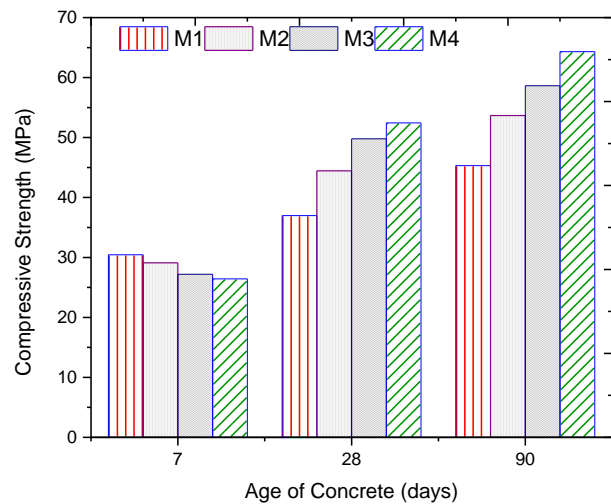
Figure 4. Compressive strength test results of control and binary mixtures

In addition to the benefits of the pozzolanic reaction, the filler effect of ultrafine RHA also plays a crucial role in strength enhancement. The fine and angular particles of ultrafine RHA improve the packing density of the concrete, filling the voids between the large size particles of cement. This filler effect contributes to a denser matrix, reducing the porosity and permeability of the concrete. The improved packing density facilitates better particle-to-particle contact and enhances the overall integrity of the concrete structure. The data in Figure 4 reveal that at 7 days, the M3 mixture (with 10% PC replaced by ultrafine RHA) exhibits about 11% lower CS

as compared to the reference mix (M1). However, at 28 and 90 days, its CS is approximately 35% and 29% higher, respectively, compared to the control mixture. Similarly, the M4 mixture (with 15% cement replaced by ultrafine RHA) shows about 13% lower strength at 7 days compared to the control mixture. Still, at 28 and 90 days, it gains about 42% and 43% higher strength, respectively, than the control mixture. These results highlight the significant contribution of ultrafine RHA towards enhancing the compressive strength of blended concrete mixtures at later ages. The delayed strength gain can be explained by the continuous pozzolanic activity, which progressively refines the concrete's microstructure and enhances its mechanical properties.

Additionally, the presence of ultrafine RHA leads to a reduction in capillary pores, which is conducive to the long-term strength development and durability of the concrete. The findings align with previous research, which also revealed that the inclusion of ultrafine RHA in concrete mixtures results in improved compressive strength at later ages [40-41]. This improvement is particularly important for applications where long-term strength and durability are critical. The use of ultrafine RHA not only addresses environmental concerns associated with the disposal of rice husks but also enhances the sustainability of concrete production by reducing the reliance on Portland cement. The scientific basis for these observations is rooted in the chemistry of the pozzolanic reaction and the resultant microstructural changes. The transformation of calcium hydroxide into C-S-H leads to a dense and cohesive matrix, which is less susceptible to cracking and other forms of deterioration. Furthermore, the angular and fine particles of ultrafine RHA improve the concrete's packing density, leading to a decline in permeability and increased resistance to aggressive environmental conditions.

3.3. Moisture Sorption

Figure 5 shows the 8-day cumulative moisture sorption test results for all the mixtures. It is noted that the incorporation of ultrafine RHA in the mixtures significantly improves the water tightness of the mixtures. Table 5 presents the percenet reduction in the 8 days cumulative moisture sorption of the modified mixtures in comparion to that of the control mixture. With increase in percent replacement of cement with ultrafine RHA, the cumulative moisture sorption of the modified mixtures is significantly reduced. The improvement in water tightness can be attributed to the pozzolanic reaction of ultrafine RHA with the hydrates of cement. This reaction results in pore filling and pore refinement within the binary concrete mixtures. The ultrafine RHA particles, due to their high fineness and reactive silica content, interact with $Ca(OH)_2$ to produce extra C-S-H [42, 43]. This C-S-H formation enhances the microstructure by reducing the size and continuity of capillary pores, thereby significantly

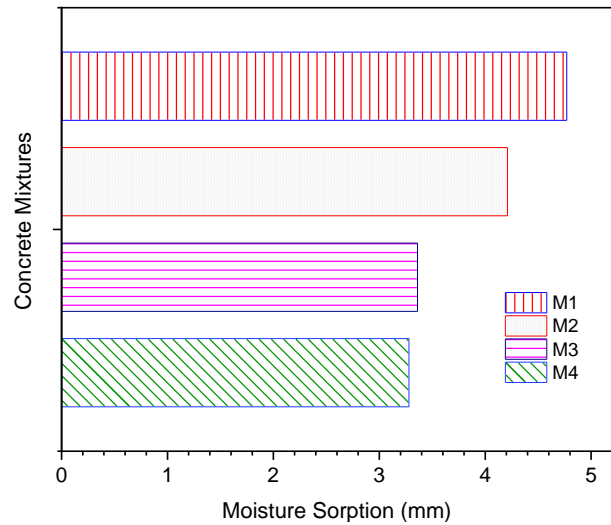increasing the moisture barrier properties of the concrete.

Figure 5. Test results of 8-day cumulative moisture sorption

Table 5. Percent Reduction in Moisture Sorption

Mix ID	Sorption Reduction (%)
M1	Reference
M2	12
M3	29
M4	31

Furthermore, the reduction in moisture sorption indicates a higher resistance to water penetration, which is crucial for the durability of concrete exposed to aggressive environments. Lower moisture sorption helps in mitigating issues related to freeze-thaw cycles, chloride ingress, and sulfate attack, thereby extending the service life of concrete structures. In addition to the chemical interactions, the physical characteristics of ultrafine RHA contribute to improved moisture resistance. The angular and fine particles of RHA enhance the packing density of the concrete matrix, leading to a more compact structure with fewer interconnected pores. This densification of the microstructure further impedes the movement of water through the concrete. The data suggests that higher ultrafine RHA content results in more significant reductions in moisture sorption [44, 45]. Specifically, M4, with the highest ultrafine RHA content, shows the greatest improvement, achieving a 31% reduction in moisture sorption compared to the control mixture. This trend highlights the potential of ultrafine RHA to substantially enhance the durability characteristics of concrete when utilized as a fractional substitution for OPC. These results are consistent with previous studies, which have demonstrated that the incorporation of pozzolanic materials such as ultrafine RHA leads to enhanced durability performance of concrete mixtures. The use of ultrafine RHA not only improves the moisture resistance of

concrete but also provides an environmentally friendly solution by utilizing agricultural waste products, thereby contributing to sustainable construction practices.

3.4. Drying Shrinkage

Shrinkage strains in concrete occur when freshly formed, moist concrete is exposed to ambient humidity, causing it to dry due to the differential relative humidity between the concrete and its surrounding environment. If the structural members made of concrete are restrained (which is usually the case), shrinkage strain can result in cracking in these members. The amount of drying shrinkage depends on several factors, including the size of the concrete member, the characteristics of the concrete constituents, and the proportion of the mixture.

For a given water-to-cement (w/cm) ratio, an increase in the cement content of the concrete mixture typically results in increased drying shrinkage [43, 46] The effect of ultrafine RHA on the critical drying shrinkage characteristic of the resulting concrete mixture was observed over 10 weeks. Figure 6 presents the test results of cumulative drying shrinkage of control and blended concrete mixtures at the 10th week of the test age. The test results show that the blended mixtures M2, M3 and M4 record reductions of about 15%, 16% and 27% in cumulative drying shrinkage, respectively when contrasted to the drying shrinkage of the reference mixture (M1). This reduction in drying shrinkage in the ultrafine RHA-blended mixtures is primarily attributed to the reduction in cement content in the binary mixtures. The lower cement content means there is less potential for shrinkage as the hydration products of cement are a major contributor to volume changes in concrete.
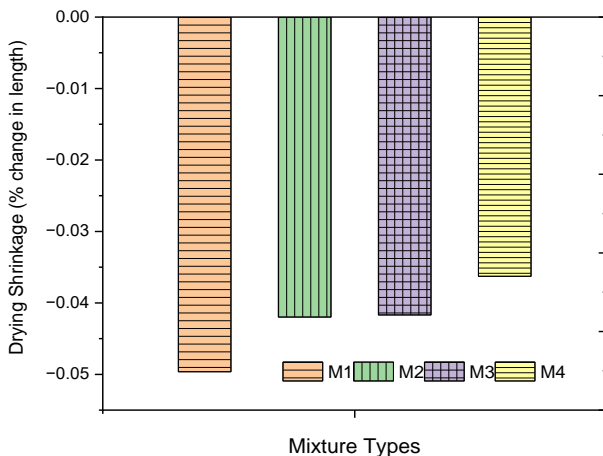

Figure 6. Cumulative drying shrinkage of control and binary mixture after 10-week

Furthermore, the ultrafine nature of RHA significantly contributes to the reduction in drying shrinkage. The incorporation of ultrafine RHA causes the production of extra C-S-H through pozzolanic reactions, which not only strengthens the concrete but also refines its pore structure. This refined pore structure reduces the overall water loss and, consequently, shrinkage [47]. Additionally, ultrafine RHA's fine and angular particles help enhance the packing density of the mix, which leads to a dense and stable matrix. This densification reduces the pathways for moisture movement, thereby decreasing the extent of drying shrinkage. The improved microstructure due to the presence of ultrafine RHA also means that the concrete has better resistance to environmental conditions that typically exacerbate shrinkage. The observed reductions in drying shrinkage for mixtures M3 and M4 are significant as they suggest that the use of ultrafine RHA can effectively mitigate one of the most common issues associated with concrete durability. By reducing shrinkage, the risk of cracking in restrained structural members is minimized, enhancing the long-term performance and integrity of the concrete [48]. These findings align with previous research, which has also reported reduced shrinkage and improved dimensional stability in concrete mixtures incorporating pozzolanic materials like ultrafine RHA.

3.5. Abrasion Mass Loss

Resistance of concrete to abrasive action, such as that from vehicular traffic on pavements, bridges, and floors, is of significant importance. The progressive loss of mass from the concrete surface due to abrasion can significantly shorten the service life of these structures. Figure 7 illustrates that the incorporation of ultrafine RHA results in a considerable enhancement of abrasion resistance in the blended concrete mixtures. At curing age of 56 days, M2, M3 and M4 concrete mixtures exhibit 7.5%, 17% and 23% decrease in loss of mass because of the abrasion, respectively, in comparison to the reference mixture (M1). This improvement in abrasion resistance is closely associated with the compressive strength of the concrete mixtures. As the compressive strength of the concrete increases, so does its ability to resist surface wear and tear caused by abrasive forces [49]. The enhancement in abrasion resistance can be attributed to several factors linked to the inclusion of ultrafine RHA. The pozzolanic reaction of ultrafine RHA with calcium hydroxide produces additional calcium silicate hydrate, which contributes to a dense and firm microstructure. This refined microstructure enhances the overall hardness and durability of the concrete surface, making it more resistant to abrasive actions. Furthermore, the angular and fine particles of ultrafine RHA contribute to the densification of the concrete matrix, reducing the number of weak points that can be worn away under abrasive forces. The improved packing density not only increases the concrete's CS but enhances its resistance to physical degradation.
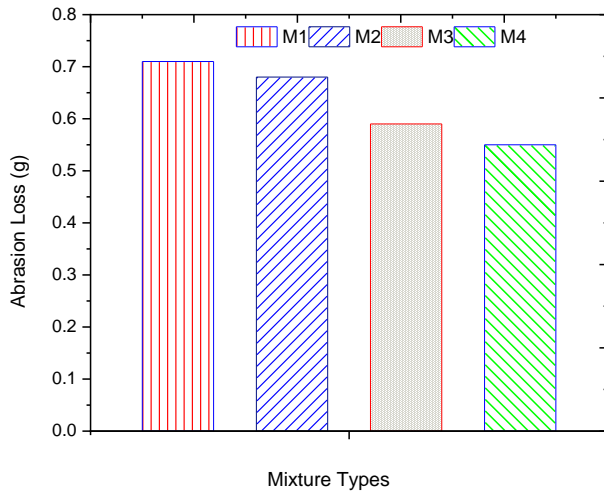
Figure 7. Mass loss due to abrasion for control and binary mixtures

In addition to the pozzolanic reaction, the filler effect of ultrafine RHA plays a crucial role in improving abrasion resistance. The fine particles of ultrafine RHA fill the voids within the concrete matrix, resulting in a denser, more cohesive structure. This improved packing density reduces the pathways through which abrasive forces can penetrate and cause damage, thereby enhancing the overall durability of the concrete. The test results follow the trend observed in the compressive strength tests, indicating that higher compressive strength generally correlates with better abrasion resistance. This relationship underscores the importance of optimizing concrete mixtures for both strength and durability to ensure long-lasting performance in abrasive environments. These findings are consistent with other studies [50, 51] that have shown the beneficial effects of incorporating supplementary cementitious materials, such as ultrafine RHA, on the abrasion resistance of concrete. The use of ultrafine RHA not only improves the mechanical properties of concrete but also provides a sustainable solution by utilizing agricultural waste, thereby contributing to environmentally friendly construction practices. The incorporation of ultrafine RHA in concrete mixtures offers significant advantages in terms of improving the durability and mechanical behavior of the material, particularly in applications where resistance to abrasion is crucial. The reduced abrasion mass loss observed in the ultrafine RHA-blended mixtures highlights the potential of ultrafine RHA as an effective supplementary binding material for improving the longevity and performance of concrete structures exposed to abrasive conditions.

3.6. Acid Resistance

Figure 8 shows the test results of acid resistance of control and binary concrete mixtures in terms of the loss in compressive strength. It is seen that compared to the control, the binary concrete mixtures show better performance (less compressive strength loss) upon exposure to H_2SO_4. After 28 days of exposure to acid, the control mix (M1) loses 24.63% of its compressive strength, while the binary mixtures M2, M3, and M4 lose 17.50%, 14.74%, and 10.6% of compressive strength, respectively. After 56 days of exposure to H_2SO_4, the loss in compressive strength for M1 (control), M2, M3, and M4 is 29%, 21.59%, 17.8%, and 12%, respectively.
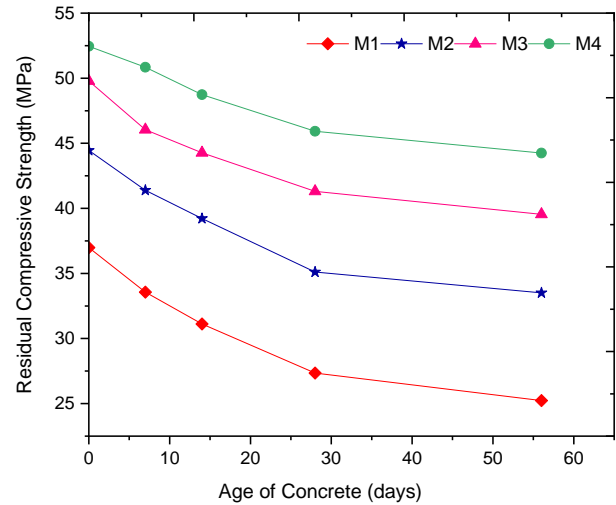
Figure 8. Progressive loss in compressive strength of mixtures during acid exposure

The blended concrete mixtures exhibit significantly less loss in compressive strength due to aging in acid in comparison to the control mix. This improved behavior against acid attack, evidenced by higher residual compressive strength, is attributed to the enhanced moisture barrier characteristics brought about by the ultrafine RHA. The results of the acid resistance test follow the trend observed in the moisture sorption test, indicating a consistent improvement in durability due to the incorporation of ultrafine RHA. The improved acid resistance of the binary concrete mixtures can be linked to the cementitious behavior of ultrafine RHA with the hydrates of binder. This reaction results in the formation of additional C-S-H, which refines the microstructure of the concrete, reducing its porosity and increasing its resistance to acid attack [52, 53]. The finer and denser microstructure impedes the ingress of aggressive agents like sulfuric acid, thereby enhancing the durability of the concrete.

Moreover, the result suggests that the acid resistance of the binary mixtures increases with the percentage replacement of PC with ultrafine RHA. The M4 mixture, with 15 wt.% replacement of PC with ultrafine RHA shows the maximum acid resistance. This trend is consistent with the findings of earlier researchers, who have reported similar improvements in the acid resistance of ultrafine RHA-blended concrete mixtures [29]. The enhanced behavior of the ultrafine RHA-blended mixtures under acidic conditions underscores the potential of ultrafine RHA as an effective SCM for improving the durability of concrete in aggressive environments. By incorporating

ultrafine RHA, the concrete not only gains improved resistance to acid attack but also contributes to sustainable construction practices by utilizing agricultural waste [54]. The findings indicate that the inclusion of ultrafine RHA in concrete mixtures could noticeably improve their resistance to acidic environments, making them more suitable for use in applications where exposure to acids is a concern. This improved performance is a testament to the beneficial effects of the pozzolanic reaction and the resulting microstructural refinement brought about by ultrafine RHA.

3.7. Scanning Electron Microscopic (SEM) Test

The Scanning Electron Microscopy images provide a detailed microstructural comparison between the control concrete mix and the concrete mix incorporating 20% ultrafine RHA. Figures 9(a) and (b) represent the SEM images of the control mix at 100 micrometers and 10 micrometers magnifications, respectively. Figures 9(c) and (d) illustrate the SEM images of the concrete mix with 20% ultrafine RHA at the same magnifications. In the SEM images of the control mix (Figures 9a and b), the microstructure shows a relatively heterogeneous and porous matrix. At the 100 micrometers magnification (Figure 9 a), large pores and cracks are evident, indicating a less dense microstructure. These pores and voids can act as pathways for water and other harmful substances, potentially leading to reduced durability and increased permeability. At the higher magnification of 10 micrometers (Figure 9b), the surface of the control mix reveals a significant amount of unreacted or partially hydrated cement particles. The presence of calcium hydroxide crystals, which are typically hexagonal plate-like structures, is noticeable. These crystals are indicative of the primary hydration product of Portland cement, which can be relatively weak and susceptible to chemical attack [28, 55]. The overall microstructure appears coarse and lacks the compactness necessary for enhanced durability.

In contrast, the SEM images of the concrete mix with 20% ultrafine RHA (Figures 9c and d) show a markedly different microstructure. At the 100 micrometers magnification (Figure 9c), the ultrafine RHA-modified mix exhibits a denser and more refined matrix. The large pores observed in the control mix are significantly reduced, indicating improved packing density and lower porosity. This densification is attributed to the pozzolanic reaction amid ultrafine RHA and $Ca(OH)_2$, resulting in the development of extra C-S-H gel, which fills the voids and cracks. At the higher magnification of 10 micrometers (Figure 9d), the microstructure of the ultrafine RHA-modified mix reveals a more uniform and compact matrix. The presence of finely distributed C-S-H gel is evident, contributing to the enhanced mechanical properties and durability of the concrete. The angular particles of ultrafine RHA appear to interlock with the cementitious matrix, further refining the pore structure and reducing the permeability [49, 52]. This refined microstructure is less susceptible to the ingress of harmful substances, thereby improving the overall resistance to chemical attack and environmental degradation.

The SEM analysis clearly demonstrates the beneficial effects of incorporating ultrafine RHA into the concrete mix. The improved microstructure, characterized by reduced porosity and enhanced densification, is a direct result of the pozzolanic activity of ultrafine RHA. This activity not only converts calcium hydroxide into C-S-H but also leads to a more compact and durable concrete matrix. The enhanced microstructural properties observed in the ultrafine RHA-modified mix correlate well with the improvements in mechanical properties and durability discussed in previous sections. This detailed SEM analysis underscores the potential of ultrafine RHA as a valuable supplementary cementitious material for producing high-performance concrete with superior durability characteristics.
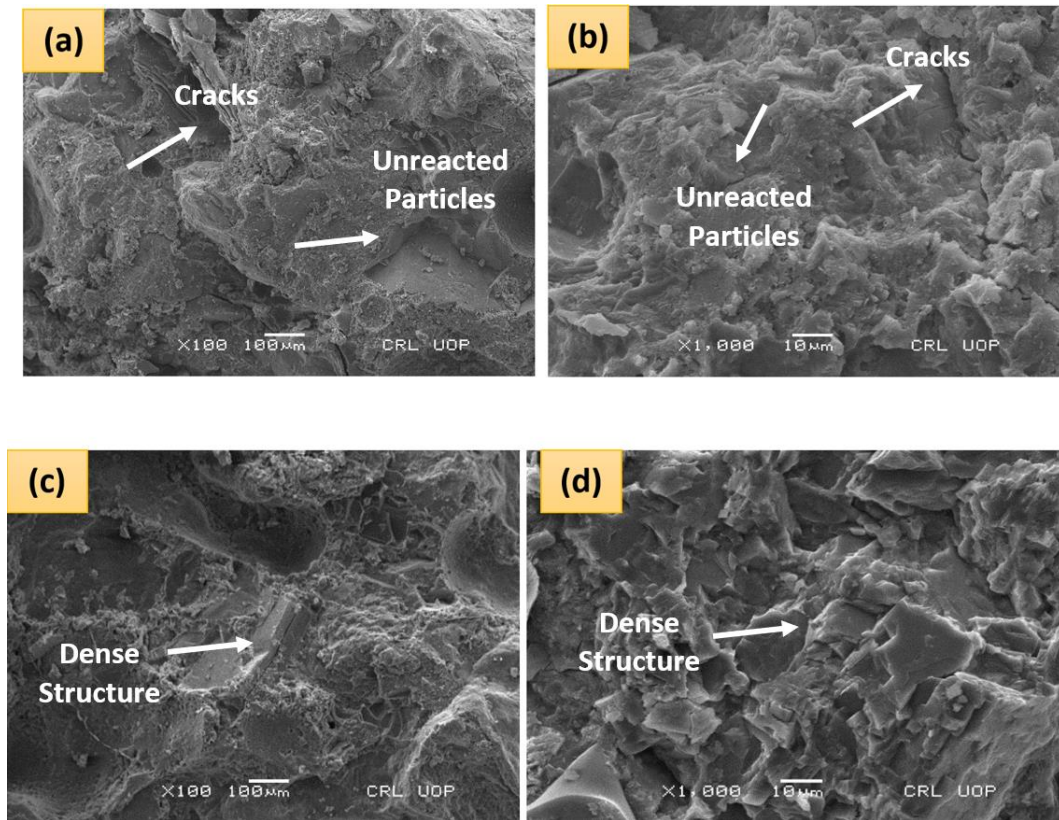
Figure 9. SEM Images of Samples: (a) Control at 100 micrometers, (b) Control at 10 micrometers, (c) Sample with 20% RHA at 100 micrometers, (b) Sample with 20% RHA at 10 micrometers

3.8. Energy Dispersive X-ray Analysis

The EDX analysis provides a detailed chemical composition of the reference mix and the mix with 20% ultrafine RHA. The EDX spectra for the control mix and the ultrafine RHA-modified mix are displayed in Figures (a) and (b), respectively, revealing significant differences in the elemental composition and distribution between the two samples. In the EDX spectrum of the control mix (Figure 10a), several key peaks are prominent. The most significant peaks correspond to oxygen (O), silicon (Si), calcium (Ca), and aluminum (Al). These elements are characteristic constituents of Portland cement and its hydration products. The oxygen peak is associated with the oxides present in the cement matrix, primarily calcium oxide (CaO) and silicon dioxide (SiO_2). The high silicon peak indicates the presence of silicates, which form the backbone of C-S-H, the primary strength-giving phase in hydrated cement paste. The calcium peak reflects the presence of calcium compounds, including Calcium oxide and Calcium hydroxide, which are integral to cement hydration. The aluminum peak suggests the inclusion of aluminate phases such as calcium aluminate (CA) and alumino-silicate phases in the cement matrix. Additionally, iron (Fe), magnesium (Mg), and sulfur (S) peaks correspond to trace elements and impurities commonly found in cement.

In contrast, the EDX spectrum of the ultrafine RHA-modified mix (Figure 10b) reveals some notable differences compared to the control mix. While the most significant peaks still correspond to oxygen (O), silicon (Si), calcium (Ca), and aluminum (Al), there are changes in the relative intensities and the appearance of additional peaks. The oxygen peak remains prominent, indicating the continued presence of oxides, but its relative intensity may be slightly altered due to the addition of ultrafine RHA. The silicon peak is more pronounced in the ultrafine RHA-modified mix, reflecting the high silica content of ultrafine RHA. This increase in silicon is indicative of the enhanced pozzolanic reaction, which contributes to additional C-S-H formation, leading to a denser and more robust microstructure. The calcium peak remains significant but is relatively reduced compared to the control mix. This reduction is due to the partial replacement of calcium-rich cement with silica-rich ultrafine RHA. The aluminum peak continues to be present, suggesting that the alumino-silicate phases are still integral to the modified matrix. The appearance of potassium (K) and sodium (Na) peaks is more noticeable in the RHA-modified mix. These elements are typically present in agricultural residues like ultrafine RHA and contribute to the overall chemical composition of the concrete [55-56].

Iron (Fe) and sulfur (S) peaks are consistent with the presence of trace elements and impurities, similar to the control mix.

The EDX analysis clearly demonstrates the impact of incorporating ultrafine RHA into the concrete mix. The increased silicon content and the altered calcium-to-silicon ratio in the ultrafine RHA-modified mix indicate a significant pozzolanic reaction, which lead to the production of extra products of hydration. This enhanced C-S-H formation improves the microstructural properties of the concrete, contributing to its increased strength and durability. The presence of potassium and sodium from the ultrafine RHA further modifies the chemical composition, potentially influencing the hydration process and the overall performance of the concrete. Overall, the EDX spectra provide a comprehensive understanding of the chemical changes induced by the incorporation of ultrafine RHA, highlighting its role in enhancing the pozzolanic behavior and improving the concrete's microstructural and durability characteristics.
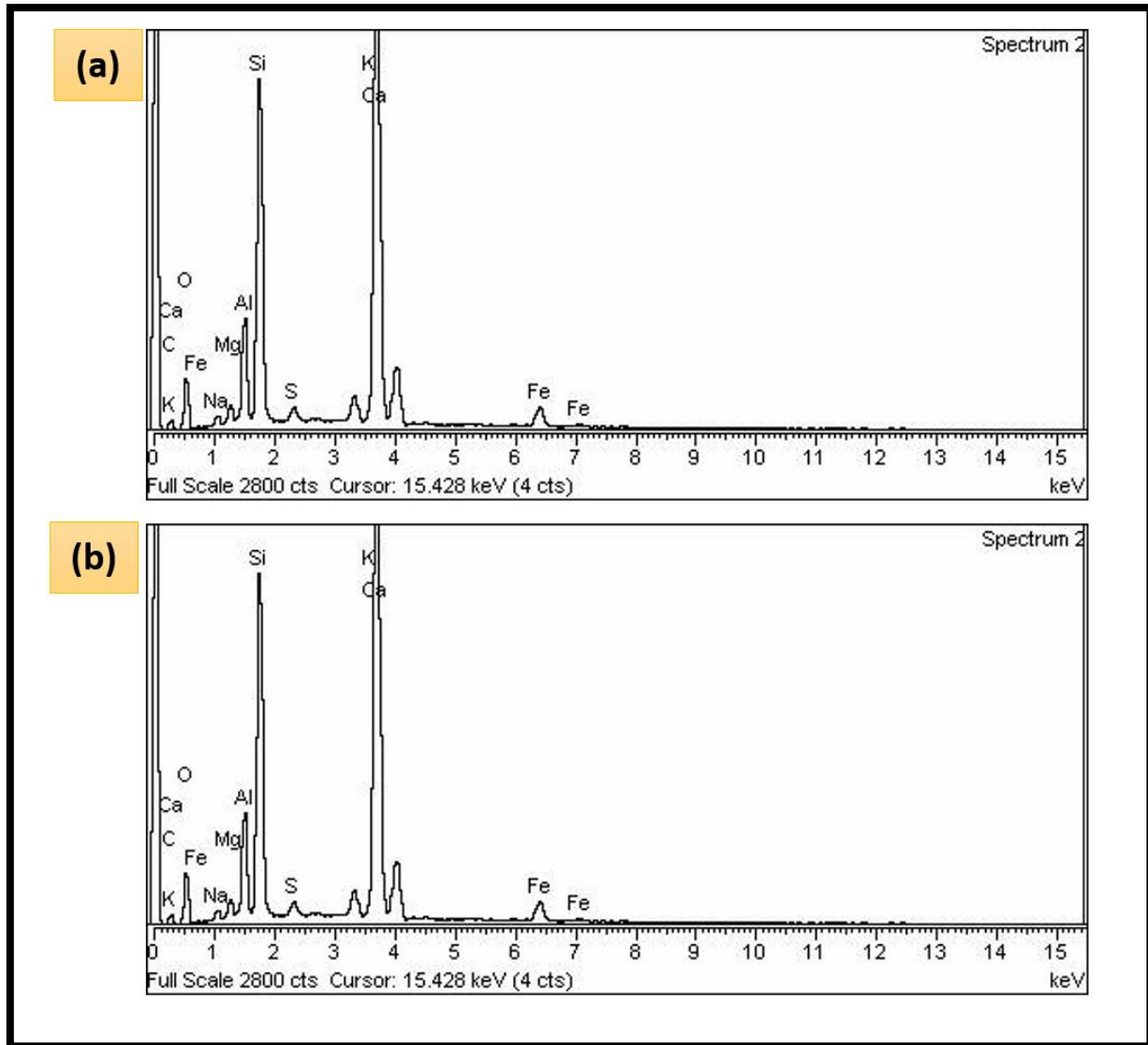

Figure 10. EDX Analysis of Samples: (a) Control, (b) Sample with 20% RHA

3.9. X-Ray Diffraction (XRD) Analysis

The XRD analysis provides key insights into the crystalline phases present in the reference mix and the mix with 20% ultrafine RHA. Figure 11 displays the XRD behavior for the reference sample and the ultrafine RHA-modified mix, respectively, highlighting significant differences in their crystalline compositions. In the XRD pattern of the control mix (Figure 11), several prominent peaks are observed, indicating the presence of well-defined crystalline phases. The most significant peaks correspond to calcium hydroxide ($Ca(OH)_2$), commonly known as portlandite, which is characterized by peaks at approximately $21°$ and $30°$. These peaks are indicative of the primary hydration product of Portland cement [28, 57]. Additionally, there are peaks corresponding to calcium silicate hydrates, though with lower intensity, suggesting that these phases are partially crystalline or amorphous. The control mix also exhibits minor peaks that may correspond to calcium carbonate ($CaCO_3$) around $49°$, which could result from carbonation on the surface of the sample.

In comparison, the XRD pattern of the ultrafine RHA-modified mix (Figure 11) reveals significant changes in comparison to the reference sample. The incorporation of 20% ultrafine RHA introduces new phases and alters the relative intensities of existing peaks. The most noticeable changes are the increased intensity of the silica (SiO_2) peak and the reduced intensity of the portlandite peaks. The pronounced peak at around $28°$ in the ultrafine RHA-modified mix indicates a high concentration of crystalline silica, which is derived from the RHA. This peak is more intense in the ultrafine RHA-modified mix, reflecting the high silica content of the ash [55].
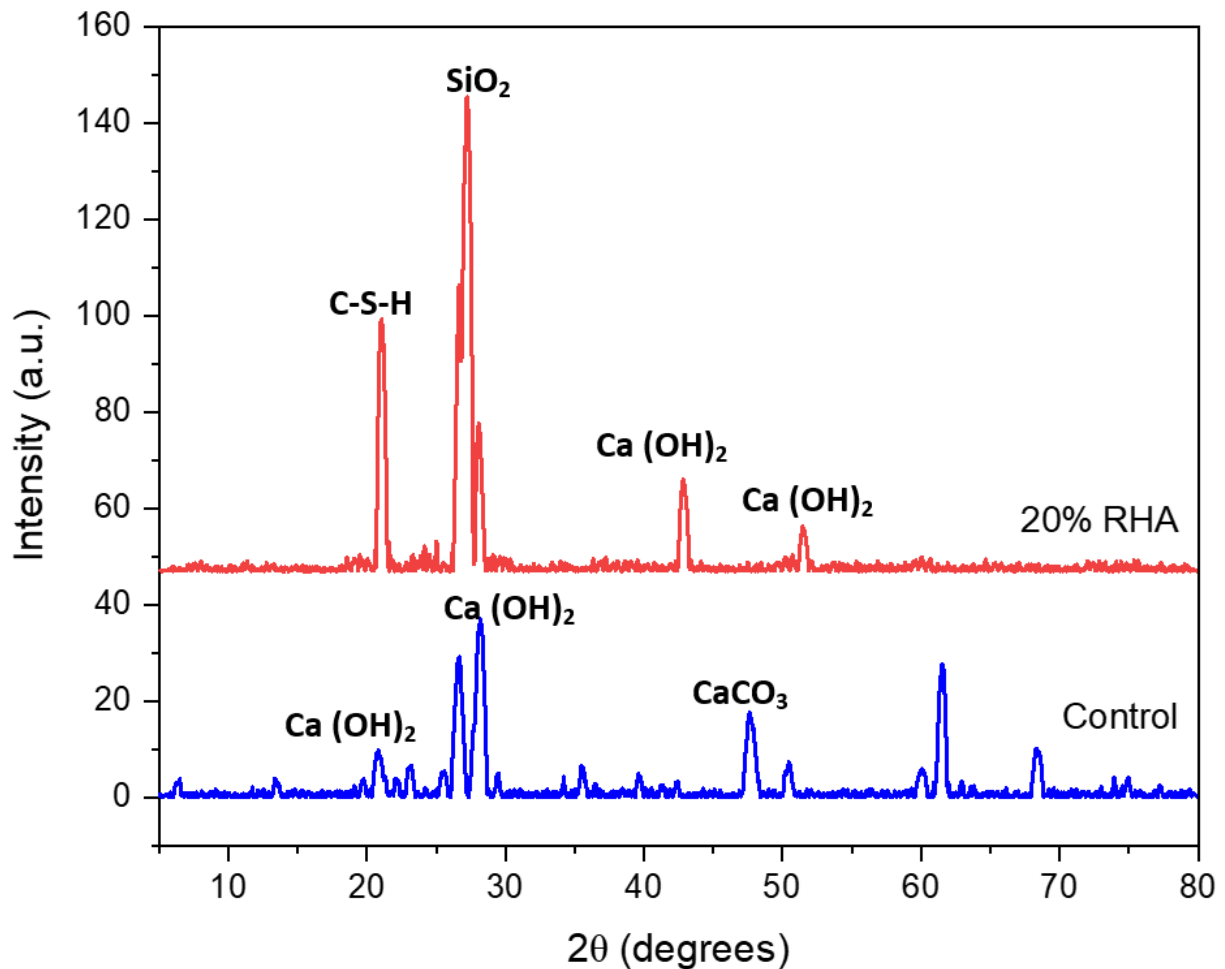

Figure 11. XRD Analysis of Samples: Control, Sample with 20% RHA

Furthermore, the peaks corresponding to portlandite are less intense in the ultrafine RHA-modified mix, suggesting a reduction in the amount of free calcium hydroxide. This reduction is due to the pozzolanic reaction between the SiO_2 in ultrafine RHA and calcium hydroxide, forming additional C-S-H. The formation of additional C-S-H phases is inferred from the overall reduction in portlandite peaks and the densification observed in the microstructure. Although C-S-H phases are often amorphous and do not produce sharp XRD peaks, their formation is supported by the reduction in free lime. The XRD analysis clearly demonstrates the impact of incorporating ultrafine RHA into the concrete mix. In the control mix, the presence of significant amounts of portlandite indicates a typical hydration process of Portland cement. However, in the ultrafine RHA-modified mix, the enhanced silica content from ultrafine RHA leads to a pozzolanic reaction, ingesting $ca(OH)_2$ and developing extra CSH. This reaction not only reduces the amount of portlandite, as evidenced by the decreased peak intensities but also increases the overall strength and durability of the concrete through the formation of more stable and denser C-S-H phases [29].

The XRD analysis supports the findings from the SEM and EDX analyses, highlighting the beneficial effects of ultrafine RHA incorporation on the microstructural and chemical properties of concrete. The increased formation of C-S-H and the reduction in free calcium hydroxide contribute to a more durable and sustainable concrete mix, making ultrafine RHA a valuable supplementary cementitious material for high-performance concrete applications. The pronounced silica peak in the ultrafine RHA-modified mix indicates the introduction of reactive silica, which is essential for the pozzolanic reaction. The reduction in portlandite peaks further confirms the effectiveness of ultrafine RHA in enhancing the pozzolanic activity, leading to improved mechanical properties and reduced porosity in the concrete matrix.

4. Conclusions

In the current research paper, each experimental analysis offered key insights into the benefits of using ultrafine RHA in concrete mixtures. The ultrafine nature of RHA, characterized by its significantly finer particle size and higher reactivity, enhances its pozzolanic activity and contributes to a denser, more durable concrete matrix. The fine particles also improve packing density and reduce porosity, which positively impacts various concrete properties. Below are the key conclusions drawn from the current study:

- The inclusion of ultrafine RHA in concrete mixtures results in a decrease in slump, indicating reduced workability. Specifically, the M3 mixture exhibited a slump of 5 cm compared to 8 cm for the control mix due to the increased surface area and water demand of ultrafine RHA particles, as well as their angular shape, which reduces fluidity.

- The compressive strength of ultrafine RHA-modified concrete mixtures significantly improves over time. The M4 mixture showed a 43% increase in compressive strength at 90 days compared to the control mix, demonstrating the beneficial pozzolanic reaction of ultrafine RHA and the filler effect, which enhances the concrete matrix density.

- Ultrafine RHA-modified mixtures exhibit enhanced water tightness. The M4 mixture recorded a 31% decrease in moisture sorption after 8 days compared to control mix, indicating improved resistance to penetration of water.

- The incorporation of ultrafine RHA reduces drying shrinkage in concrete mixtures. The M4 mixture showed a 27% reduction in cumulative drying shrinkage over 10 weeks compared to the control mix due to the denser microstructure, refined pore structure, and reduced cement content, which collectively minimize water loss and shrinkage.

- Ultrafine RHA enhances the abrasion resistance of concrete. The M4 mixture exhibited a 23% decrease in loss of mass because of the abrasion at 56 days in comparison to the reference mix. This improvement is attributed to the increased compressive strength, denser microstructure, and better packing density provided by the fine and angular particles of ultrafine RHA.

- Ultrafine RHA-modified concrete shows improved resistance to acid attack. The M4 mixture lost only 12% of its compressive strength after 56 days of exposure to H_2SO_4, compared to a 29% loss in the control mix. This resistance is due to the refined microstructural and increased formation of products of hydration, which provide better durability against acidic environments.

- The SEM images revealed a denser and more refined microstructure in the ultrafine RHA-modified mix. The number of large pores and cracks was significantly reduced, contributing to the improved mechanical properties and durability of the concrete. The presence of fine RHA particles filled voids and enhanced the overall compactness of the concrete matrix.

- The EDX spectra confirmed the increased silica content and reduced calcium hydroxide in the ultrafine RHA-modified mix. The relative intensity of the silica peak in the RHA mix was significantly higher, indicating enhanced pozzolanic activity.

- The XRD patterns demonstrated a reduction in portlandite peaks and an increase in silica peaks in the ultrafine RHA-modified mix. The pronounced silica peak at around 26° and reduced portlandite peaks confirmed the formation of additional C-S-H, enhancing the concrete's strength and durability.

In conclusion, the incorporation of ultrafine RHA as a

partial replacement for cement in concrete significantly enhances various properties, including compressive strength, moisture resistance, abrasion resistance, and acid resistance. The pozzolanic activity of ultrafine RHA plays a crucial role in these improvements, making it a valuable supplementary cementitious material for sustainable and high-performance concrete applications.

List of Abbreviations

RHA (Rice Husk Ash), SEM (Scanning Electron Microscopy), EDX (Energy Dispersive X-ray), XRD (X-ray Diffraction), PC (Portland Cement), C-S-H (Calcium Silicate Hydrate), $Ca(OH)_2$ (Calcium Hydroxide), H_2SO_4 (Sulfuric Acid), $CaCO_3$ (Calcium Carbonate), wt.% (Weight Percent)

Declarations

Availability of Data and Material

All data generated or analyzed during this study are included in this published article [and its supplementary information files].

Competing Interests

The authors have no relevant financial or non-financial interests to disclose.

Authors' Contributions

Roz-Ud-Din Nassar: conceptualization, draft checking, editing, data curation, and supervision

Shah room: testing, data curation, draft writing, and coordination

REFERENCES

[1]   A. Liu, D. Kong, J. Jiang, L. Wang, C. Liu, and R. He, "Mechanical properties and microscopic mechanism of basalt fiber-reinforced red mud concrete," *Constr Build Mater*, vol. 416, p. 135155, 2024, doi:https://doi.org/10.1016/j.conbuildmat.2024.135155.

[2]   Y. Wang *et al.*, "Deterioration mechanism and hardness degradation for GFRP bars used in marine concrete structures," *Case Studies in Construction Materials*, vol. 20, p. e02932, 2024, doi:https://doi.org/10.1016/j.cscm.2024.e02932.

[3]   C. Tang *et al.*, "Effects of shrinkage reducing admixture and internal curing agent on shrinkage and creep of high performance concrete," *Journal of Building Engineering*, vol. 71, p. 106446, 2023, doi: https://doi.org/10.1016/j.jobe.2023.106446.

[4]   A. Hassan, A. ElNemr, L. Goebel, and C. Koenke, "Effect of hybrid polypropylene fibers on mechanical and shrinkage behavior of alkali-activated slag concrete," *Construction and Building Materials*, vol. 411, p. 134485, 2024, doi: https://doi.org/10.1016/j.conbuildmat.2023.134485.

[5]   G. Ke, J. Zhang, and Y. Liu, "Shrinkage characteristics of calcium sulphoaluminate cement concrete," *Construction and Building Materials*, vol. 337, p. 127627, 2022, doi: https://doi.org/10.1016/j.conbuildmat.2022.127627.

[6]   E. H. A. H. M. Shameer Saleh Ying-Lei Li and X.-L. Zhao, "Workability, strength, and shrinkage of ultra-high-performance seawater, sea sand concrete with different OPC replacement ratios," *Journal of Sustainable Cement-Based Materials*, vol. 12, no. 3, pp. 271–291, 2023, doi: 10.1080/21650373.2022.2050831.

[7]   S. Saleh, Y.-L. Li, E. Hamed, A. H. Mahmood, and X.-L. Zhao, "Workability, strength, and shrinkage of ultra-high-performance seawater, sea sand concrete with different OPC replacement ratios," *Journal of Sustainable Cement-Based Materials*, vol. 12, no. 3, pp. 271–291, 2023, doi: 10.1080/21650373.2022.2050831.

[8]   A. Aneja, R. L. Sharma, and H. Singh, "Mechanical and durability properties of biochar concrete," *Materials Today: Proceedings*, vol. 65, pp. 3724–3730, 2022, doi: https://doi.org/10.1016/j.matpr.2022.06.371.

[9]   T. A. Abdalla, D. O. Koteng, S. M. Shitote, and M. Matallah, "Mechanical and durability properties of concrete incorporating silica fume and a high volume of sugarcane bagasse ash," *Results in Engineering*, vol. 16, p. 100666, 2022, doi: https://doi.org/10.1016/j.rineng.2022.100666.

[10]   M. Wasim, A. Abadel, B. H. Abu Bakar, and I. M. H. Alshaikh, "Future directions for the application of zero carbon concrete in civil engineering – A review," *Case Studies in Construction Materials*, vol. 17, p. e01318, 2022, doi: https://doi.org/10.1016/j.cscm.2022.e01318.

[11]   N. J. Mim *et al.*, "Eco-friendly and cost-effective self-compacting concrete using waste banana leaf ash," *Journal of Building Engineering*, vol. 64, p. 105581, 2023, doi: https://doi.org/10.1016/j.jobe.2022.105581.

[12]   H. M. Tuncer and Z. C. Girgin, "Hemp Fiber Reinforced Lightweight Concrete (HRLWC) with Supplementary Cementitious Materials (SCM)," Building for the Future: Durable, Sustainable, Resilient. fib Symposium 2023. Lecture Notes in Civil Engineering, vol. 349, 2023, pp. 1067–1074. doi: 10.1007/978-3-031-32519-9_107.

[13]   C. Dong *et al.*, "Fresh and hardened properties of recycled plastic fiber reinforced self-compacting concrete made with recycled concrete aggregate and fly ash, slag, silica fume," *Journal of Building Engineering*, vol. 62, p. 105384, 2022,

doi: https://doi.org/10.1016/j.jobe.2022.105384.

[14] M. Gesoğlu, E. Güneyisi, and E. Özbay, "Properties of self-compacting concretes made with binary, ternary, and quaternary cementitious blends of fly ash, blast furnace slag, and silica fume," *Construction and Building Materials*, vol. 23, no. 5, pp. 1847–1854, 2009, doi:https://doi.org/10.1016/j.conbuildmat.2008.09.015.

[15] E.-H. Yang, Y. Yang, and V. Li, "Use of High Volumes of Fly Ash to Improve ECC Mechanical Properties and Material Greenness," *ACI Materials Journal*, vol. 104, pp. 620–628, 2007.

[16] Y. Wang, T. Zheng, X. Zheng, Y. Liu, J. Darkwa, and G. Zhou, "Thermo-mechanical and moisture absorption properties of fly ash-based lightweight geopolymer concrete reinforced by polypropylene fibers," *Construction and Building Materials*, vol. 251, p. 118960, 2020, doi: https://doi.org/10.1016/j.conbuildmat.2020.118960.

[17] M. Golias, J. Castro, and J. Weiss, "The influence of the initial moisture content of lightweight aggregate on internal curing," *Construction and Building Materials*, vol. 35, pp. 52–62, 2012, doi: https://doi.org/10.1016/j.conbuildmat.2012.02.074.

[18] K.-H. Yang, Y.-B. Jung, M.-S. Cho, and S.-H. Tae, "Effect of supplementary cementitious materials on reduction of CO2 emissions from concrete," *J Clean Prod*, vol. 103, pp. 774–783, 2015, doi: https://doi.org/10.1016/j.jclepro.2014.03.018.

[19] R. Infante Gomes, C. Brazão Farinha, R. Veiga, J. de Brito, P. Faria, and D. Bastos, "CO2 sequestration by construction and demolition waste aggregates and effect on mortars and concrete performance - An overview," *Renewable and Sustainable Energy Reviews*, vol. 152, p. 111668, 2021, doi: https://doi.org/10.1016/j.rser.2021.111668.

[20] K.-H. Yang, J. Song, and K.-I. Song, "Assessment of CO2 reduction of alkali-activated concrete," *J Clean Prod*, vol. 39, pp. 265–272, 2013, doi: 10.1016/j.jclepro.2012.08.001.

[21] J. Liu, G. Liu, W. Zhang, Z. Li, H. Jin, and F. Xing, "A new approach to CO2 capture and sequestration: A novel carbon capture artificial aggregates made from biochar and municipal waste incineration bottom ash," *Constr Build Mater*, vol. 398, p. 132472, 2023, doi: https://doi.org/10.1016/j.conbuildmat.2023.132472.

[22] M. A. Yahya, Z. Al-Qodah, and C. W. Z. Ngah, "Agricultural bio-waste materials as potential sustainable precursors used for activated carbon production: A review," *Renewable and Sustainable Energy Reviews*, vol. 46, pp. 218–235, 2015, doi: https://doi.org/10.1016/j.rser.2015.02.051.

[23] S. N. Chinnu, S. N. Minnu, A. Bahurudeen, and R. Senthilkumar, "Reuse of industrial and agricultural by-products as pozzolan and aggregates in lightweight concrete," *Constr Build Mater*, vol. 302, p. 124172, 2021, doi: https://doi.org/10.1016/j.conbuildmat.2021.124172.

[24] G. Tatrari *et al.*, "Mass production of metal-doped graphene from the agriculture waste of Quercus ilex leaves for supercapacitors: inclusive DFT study," *RSC Adv.*, vol. 11, no. 18, pp. 10891–10901, 2021, doi: https://doi.org/10.1039/D0RA09393A.

[25] I. Y. Hakeem, M. Amin, I. S. Agwa, M. H. Abd-Elrahman, and M. F. Abdelmagied, "Using a combination of industrial and agricultural wastes to manufacture sustainable ultra-high-performance concrete," *Case Studies in Construction Materials*, vol. 19, p. e02323, 2023, doi: https://doi.org/10.1016/j.cscm.2023.e02323.

[26] M. A. Khan, S. Ayub Khan, B. Khan, K. Shahzada, F. Althoey, and A. F. Deifalla, "Investigating the feasibility of producing sustainable and compatible binder using marble waste, fly ash, and rice husk ash: A comprehensive research for material characteristics and production," *Results in Engineering*, vol. 20, p. 101435, 2023, doi: https://doi.org/10.1016/j.rineng.2023.101435.

[27] A. Kashem, R. Karim, P. Das, S. Datta, and M. Alharthai, "Compressive strength prediction of sustainable concrete incorporating rice husk ash (RHA) using hybrid machine learning algorithms and parametric analyses," *Case Studies in Construction Materials*, vol. 20, p. e03030, 2024, doi: 10.1016/j.cscm.2024.e03030.

[28] A. G. Díaz, S. Bueno, L. P. Villarejo, and D. Eliche-Quesada, "Improved strength of alkali activated materials based on construction and demolition waste with addition of rice husk ash," *Construction and Building Materials*, vol. 413, p. 134823, 2024, doi: https://doi.org/10.1016/j.conbuildmat.2023.134823.

[29] F. Althoey *et al.*, "Impact of sulfate activation of rice husk ash on the performance of high strength steel fiber reinforced recycled aggregate concrete," *Journal of Building Engineering*, vol. 54, p. 104610, 2022, doi: https://doi.org/10.1016/j.jobe.2022.104610.

[30] O. Zaid, J. Ahmad, M. S. Siddique, and F. Aslam, "Effect of Incorporation of Rice Husk Ash Instead of Cement on the Performance of Steel Fibers Reinforced Concrete," *Frontiers in Materials*, vol. 8, pp. 14–28, 2021, doi: doi: 10.3389/fmats.2021.665625.

[31] M. S. Mahmood *et al.*, "Enhancing compressive strength prediction in self-compacting concrete using machine learning and deep learning techniques with incorporation of rice husk ash and marble powder," *Case Studies in Construction Materials*, vol. 19, p. e02557, 2023, doi: https://doi.org/10.1016/j.cscm.2023.e02557.

[32] A. P. Vieira, R. D. Toledo Filho, L. M. Tavares, and G. C. Cordeiro, "Effect of particle size, porous structure and content of rice husk ash on the hydration process and compressive strength evolution of concrete," *Constr Build Mater*, vol. 236, p. 117553, 2020.

[33] P. J. Ramadhansyah *et al.*, "Strength and Porosity of Porous Concrete Pavement Containing Nano Black Rice Husk Ash," in *IOP Conference Series: Materials Science and Engineering*, IOP Publishing, 2020, p. 12037.

[34] ASTM C150, "Standard Specification for Portland Cement," 2017.

[35] ASTM C192, "Standard Practice for Making and Curing Concrete Test Specimens in the Laboratory," 2015.

[36] ASTM C157-75, "Standard Test Method for Length Change of Hardened Cement Mortar and Concrete."

[37] ASTM C490, "Standard Practice for Use of Apparatus for the Determination of Length Change of Hardened Cement Paste, Mortar, and Concrete."

[38] ASTM C1898-20, "Standard Test Methods for Determining the Chemical Resistance of Concrete Products to Acid Attack, ASTM International, West Conshohocken, PA," 2020.

[39] S. A. Memon, M. A. Shaikh, and H. Akbar, "Utilization of Rice Husk Ash as viscosity modifying agent in Self Compacting Concrete," *Construction and Building Materials*, vol. 25, no. 2, pp. 1044–1048, 2011, doi: https://doi.org/10.1016/j.conbuildmat.2010.06.074.

[40] M. Vigneshwari, K. Arunachalam, and A. Angayarkanni, "Replacement of silica fume with thermally treated rice husk ash in Reactive Powder Concrete," *Journal of Cleaner Production*, vol. 188, pp. 264–277, 2018, doi: https://doi.org/10.1016/j.jclepro.2018.04.008.

[41] E. Mohseni, M. J. Kazemi, M. Koushkbaghi, B. Zehtab, and B. Behforouz, "Evaluation of mechanical and durability properties of fiber-reinforced lightweight geopolymer composites based on rice husk ash and nano-alumina," *Construction and Building Materials*, vol. 209, pp. 532–540, 2019, doi: https://doi.org/10.1016/j.conbuildmat.2019.03.067.

[42] S.-H. Kang, S.-G. Hong, and J. Moon, "The use of rice husk ash as reactive filler in ultra-high performance concrete," *Cement and Concrete Research*, vol. 115, pp. 389–400, 2019, doi: https://doi.org/10.1016/j.cemconres.2018.09.004.

[43] V.-T.-A. Van, C. Rößler, D.-D. Bui, and H.-M. Ludwig, "Rice husk ash as both pozzolanic admixture and internal curing agent in ultra-high performance concrete," *Cement and Concrete Composites*, vol. 53, pp. 270–278, 2014, doi: https://doi.org/10.1016/j.cemconcomp.2014.07.015.

[44] S. A. Zareei, F. Ameri, F. Dorostkar, and M. Ahmadi, "Rice husk ash as a partial replacement of cement in high strength concrete containing micro silica: Evaluating durability and mechanical properties," *Case Studies in Construction Materials*, vol. 7, pp. 73–81, 2017, doi: https://doi.org/10.1016/j.cscm.2017.05.001.

[45] H. Huang, X. Gao, H. Wang, and H. Ye, "Influence of rice husk ash on strength and permeability of ultra-high performance concrete," *Construction and Building Materials*, vol. 149, pp. 621–628, 2017, doi: https://doi.org/10.1016/j.conbuildmat.2017.05.155.

[46] S. Muthukrishnan, S. Gupta, and H. W. Kua, "Application of rice husk biochar and thermally treated low silica rice husk ash to improve physical properties of cement mortar," *Theoretical and Applied Fracture Mechanics*, vol. 104, p. 102376, 2019, doi: https://doi.org/10.1016/j.tafmec.2019.102376.

[47] C. Fapohunda, B. Akinbile, and A. Shittu, "Structure and properties of mortar and concrete with rice husk ash as partial replacement of ordinary Portland cement – A review," *International Journal of Sustainable Built Environment*, vol. 6, no. 2, pp. 675–692, 2017, doi: https://doi.org/10.1016/j.ijsbe.2017.07.004.

[48] J. Wang, J. Xiao, Z. Zhang, K. Han, X. Hu, and F. Jiang, "Action mechanism of rice husk ash and the effect on main performances of cement-based materials: A review," *Construction and Building Materials*, vol. 288, p. 123068, 2021, doi: https://doi.org/10.1016/j.conbuildmat.2021.123068.

[49] W. Zhang, H. Liu, and C. Liu, "Impact of Rice Husk Ash on the Mechanical Characteristics and Freeze–Thaw Resistance of Recycled Aggregate Concrete," *Applied Sciences*, vol. 12, no. 23, 2022, doi: 10.3390/app122312238.

[50] B. Ambedkar, J. Alex, and J. Dhanalakshmi, "Enhancement of mechanical properties and durability of the cement concrete by RHA as cement replacement: Experiments and modeling," *Construction and Building Materials*, vol. 148, pp. 167–175, 2017, doi: https://doi.org/10.1016/j.conbuildmat.2017.05.022.

[51] F. B. Witzke, N. A. M. Beltrame, C. Angulski da Luz, and R. A. Medeiros-Junior, "Abrasion resistance of metakaolin-based geopolymers through accelerated testing and natural wear," *Wear*, vol. 530–531, p. 204996, 2023, doi: https://doi.org/10.1016/j.wear.2023.204996.

[52] T. R. Praveenkumar, M. M. Vijayalakshmi, and M. S. Meddah, "Strengths and durability performances of blended cement concrete with TiO2 nanoparticles and rice husk ash," *Construction and Building Materials*, vol. 217, pp. 343–351, 2019, doi: https://doi.org/10.1016/j.conbuildmat.2019.05.045.

[53] B. A. Tayeh, R. Alyousef, H. Alabduljabbar, and A. Alaskar, "Recycling of rice husk waste for a sustainable concrete: A critical review," *Journal of Cleaner Production*, vol. 312, p. 127734, 2021, doi: https://doi.org/10.1016/j.jclepro.2021.127734.

[54] L. A. Qureshi, B. Ali, and A. Ali, "Combined effects of supplementary cementitious materials (silica fume, GGBS, fly ash and rice husk ash) and steel fiber on the hardened properties of recycled aggregate concrete," *Construction and Building Materials*, vol. 263, p. 120636, 2020, doi: https://doi.org/10.1016/j.conbuildmat.2020.120636.

[55] C. Liu *et al.*, "Recycled aggregate concrete with the incorporation of rice husk ash: Mechanical properties and microstructure," *Construction and Building Materials*, vol. 351, p. 128934, 2022, doi: https://doi.org/10.1016/j.conbuildmat.2022.128934.

[56] M. M. Meraz *et al.*, "Using rice husk ash to imitate the properties of silica fume in high-performance fiber-reinforced concrete (HPFRC): A comprehensive durability and life-cycle evaluation," *Journal of Building Engineering*, vol. 76, p. 107219, 2023, doi: https://doi.org/10.1016/j.jobe.2023.107219.

[57] R. Siddique, K. Singh, Kunal, M. Singh, V. Corinaldesi, and A. Rajor, "Properties of bacterial rice husk ash concrete," *Construction and Building Materials*, vol. 121, pp. 112–119, 2016, doi: https://doi.org/10.1016/j.conbuildmat.2016.05.146.